Fusion Engineering and Design. Volume 127, February 2018, Pages 127-138, ISSN 0920-3796,

https://doi.org/10.1016/j.fusengdes.2017.12.018

The LIPAc beam dump

Beatriz Brañas[a,*], Fernando Arranz[a], Oriol Nomen[b], Daniel Iglesias[a], Francisco Ogando[c], Marcos Parro[a], Jesús Castellanos[a], Joaquín Mollá[a], Concepción Oliver[a], David Rapisarda[a], Patrick Sauvan[c]

[a] *CIEMAT, Avda. Complutense 22, 28040 Madrid, Spain*
[b] *IREC, Jardins de les Dones de Negre, 1, 2ª, 08930, Sant Adrià de Besòs, Barcelona, Spain*
[c] *Dpto. de Ingeniería Energética, ETSII-UNED, C/Juan del Rosal, 12, 28040, Madrid, Spain*

Abstract

The International Fusion Materials Irradiation Facility (IFMIF) aims to provide an accelerator-based, D-Li neutron source to produce high energy neutrons at sufficient intensity and irradiation volume for fusion materials qualification. The LIPAc is a 125 mA 9 MeV continuous wave deuteron accelerator whose components are under construction mainly in Europe, which is being installed in Rokkasho (Japan) with the purpose of validating the IFMIF accelerator design.

The beam generated by the LIPAc accelerator will be stopped by a copper cone (2.5 m long, 6.8° angle), cooled by water flowing at high velocity along its outer surface. This piece is surrounded by a shield made of iron and low Z materials for attenuating the neutron and gamma radiation originated by the interaction of the deuterons with the copper. It incorporates dedicated diagnostics for beam dump monitoring: accelerometers for detection of localized heating due to incorrect alignment of the beam and ionization chambers, which ensure that the deuteron beam footprint remains within the beam dump design limits.

A lead shutter has been designed to be inserted in the beam tube during beam-off periods to stop the gamma radiation from the activated copper cone escaping through the beam tube, allowing access inside the accelerator vault. The junction of the beam dump to the beam tube has a special design to allow its remote disconnection, enabling the end of life decommissioning operations of the facility. The design and material selection of the beam dump and neighboring elements are driven by a maintenance-free requirement after a short period of operations, as the cartridge activation precludes any maintenance activities in the beam dump and neighboring elements downstream the lead shutter.

This paper describes the design and manufacturing of the beam dump and related elements explaining the interrelations between them and the reasons behind their main features.

Keywords:

Beam dump, Ion accelerator, Particle beam handling

1. Introduction

The International Fusion Materials Irradiation Facility, also known as IFMIF, will be a test facility for the qualification of fusion reactors candidate materials [1]. The LIPAc (Linear IFMIF Prototype Accelerator) [2,3] is a prototype accelerator (9 MeV, 125 mA of D+ beam in continuous wave), identical to the low energy part of one of the two IFMIF accelerators. The LIPAc will not have a target and hence a dump [4,5] is needed to stop the deuteron beam.

The LIPAc beam dump design and manufacturing represents a challenge because it must stop safely the deuteron beam with a continuous power of 1.125 MW which has no precedent in any other linear accelerator. The LIPAc beam is opened at the end of the accelerator with a beam expander made of three quadrupoles giving a beam at the beam dump entrance with a rms size of 40 mm and divergences of 15 mrad in horizontal direction and 17 mrad in vertical direction.

The beam dump has been designed carefully considering the characteristics of the LIPAc beam and assuring that the temperature and thermomechanical stresses in the material during the accelerator operation are inside acceptable values. The use of deuterons poses additional difficulties due to the fact that the interaction of 9 MeV deuterons with any material lead to neutron generation and also to the material activation. This last point makes maintenance operations not possible after few hours of full power operation and consequently determines many of the design features.

The radiation field during operation forces a careful selection of materials in the accelerator, especially in the beam dump and last part of the transport line where components must be metallic if possible or radiation resistant plastics. The estimated maximum absorbed doses, which vary from 10^3–10^5 Gy around the beam tube depending on the distance to the accelerator axis and to the beam dump, up to $5{\cdot}10^6$ Gy inside the beam dump shield, have been taken into account in the selection of the different materials (for magnet elements like resins or isolators, vacuum gaskets, hydraulic fittings, pneumatic mechanisms, etc.).

The beam dump system includes the following components (see Fig. 1):

- Cartridge which is the beam stopping piece, cooled by water

- Shield surrounding the cartridge

- Cooling system

- Connection to the beam line

The vacuum pumping is provided by cryopumps located in the accelerator line outside the beam dump shield which guarantee a pressure inside the beam dump and neighboring chambers in the order of 10^{-5} mbar during full power operation.

In the following sections, the description of each of the previously listed components is presented with emphasis on the design aspects and showing also the ongoing manufacturing status.

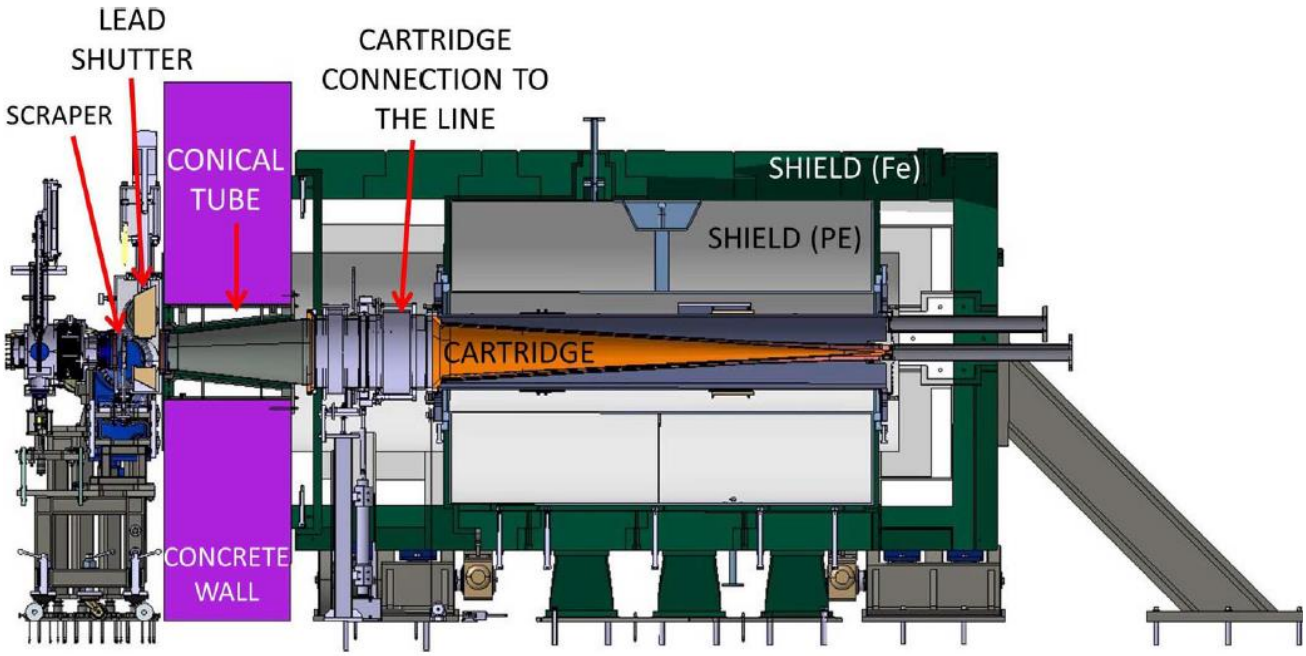

Figure 1. Beam Dump section showing the main elements.

2. Cartridge

2.1. Description

The beam dump cartridge (Fig. 2) is constituted by the following main components:

- The cone, which is the piece where the beam is stopped,

- A shroud, concentric with the cone to provide the path for the high velocity coolant flow

- The cylinder and rear flange, which is the mechanical support of the previous pieces

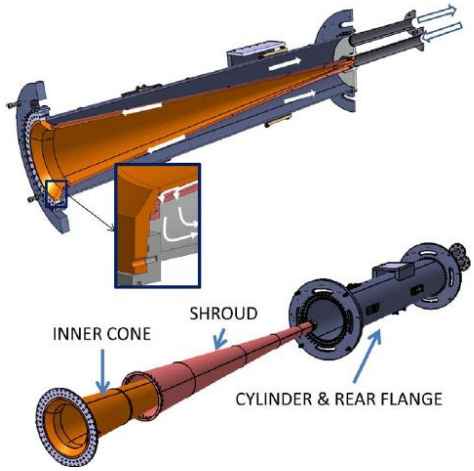

Figure 2 Beam dump cartridge. The different parts and the water path are showed.

These components are mounted according to the scheme shown in Fig. 2. The three pieces are joined at the cone flange leaving the tip of the cone free to displace axially due to the thermal expansion (the expected displacement is 3.7 mm).

The inner cone (2500 mm length, 6.8° opening angle, 5–6.5 mm thickness) is made of copper and cooled by high velocity water flowing along its outer surface. Although other optimized geometries could lead to lower power density values, the conical geometry provides the minimum thermal stresses as it is explained in [3,6]. While the cone length was established from space availability criteria, the angle was chosen to contain the nominal beam taking into account margin for beam errors while obtaining manageable power density values (below 3 MW/m^2) and not too high radiation leak through the cone aperture. The small thickness was defined to minimize the temperature difference between inner and outer surface and thus the thermal stresses, while providing enough stiffness against buckling. A study comparing different materials was performed including mechanical, radioprotection and manufacturability aspects, being the final choice of copper as beam dump material driven mainly by its thermomechanical response.

The cone has a 40 mm long 45° chamfer at the aperture to absorb particles from the beam halo or from off-normal beams. It finishes in a stainless steel-copper flange which allows the connection to the rest of the line using an helicoflex joint against the stainless steel surface.

The cooling water flows along the outer surface of the cone, through the annular channel formed between the cone and the shroud, which is also made of copper. The shroud has an apparently conical geometry but it is in reality made of four truncated cones with slightly different slopes which ensure a high velocity of the water and consequently a high heat transfer in the central region of the beam dump where the power deposition is maximum [4]. After cooling the cone the water crosses the shroud (see detail in Fig. 2) and returns through the space between the shroud and a stainless steel cylinder.

2.2. Cooling and thermomechanical analysis

The cooling of the cartridge has been designed with the following requirements:

- The coolant must be liquid water. The pressure at the inlet must guarantee such condition.

- Copper temperature design limit has been established at 150 °C.

- The inlet pressure must be such that no buckling issues in the long and thin inner cone arise.

- Avoid high erosion in the cooling channel. The velocity must be high enough to cool down the piece without reaching locally saturation temperatures but not too high, to avoid erosion phenomena.

- The maximum temperatures at the water-copper interface should be close to the saturation point with the aim of allowing the detection of abnormal beam conditions that could represent a risk for the beam dump by bubble noise monitoring [7,8].

The water flows through the beam dump cooling channel with a velocity between 4 m/s and 10 m/s depending on the region. The cooling system parameters (pressure of 3.5 bar at the beam dump entrance, flow rate of 30 kg/s) and the geometry of the cooling channel (5.5–7mm width, surface roughness greater than 6.5 micrometers) were obtained from a 1D analysis plus 3D simulations with Ansys/CFX in the regions of the cooling channel near the tip and flange [7]. The design allows deviations from the nominal conditions, being the critical heat flux at least twice the nominal beam heat flux.

Experiments have been performed on a 1:1 prototype of the cartridge [8,9] with a hydraulic test circuit providing a water flow with the parameters required for the LIPAc beam dump. A pressure loss in the cartridge of 1.5 bar was measured, in agreement with the theoretical estimations. Also the stability of the beam dump against vibrations induced by the coolant flow was checked experimentally and numerically [10].

The heat transfer coefficient values used in the simulations influence significantly the obtained results and in particular the temperature of the copper in contact with the water and therefore the margin to boiling. These values are also used as contour condition for the mechanical analyses. Pethukov correlation was selected because its adequacy to the beam dump conditions (annular channel, temperature differences between wall and water in the order of 10 degrees). The film coefficients obtained from this correlation were found to be consistent with those deduced from the fluid-dynamic calculations with the SST turbulence model. An experimental validation was performed using a prototype of the cooling channel equipped with a heater and thermocouples in the same hydraulic test circuit mentioned above. Taking into account experimental uncertainties, the measured values of the heat transfer coefficient are in agreement with those derived from the correlations (see Fig. 3).

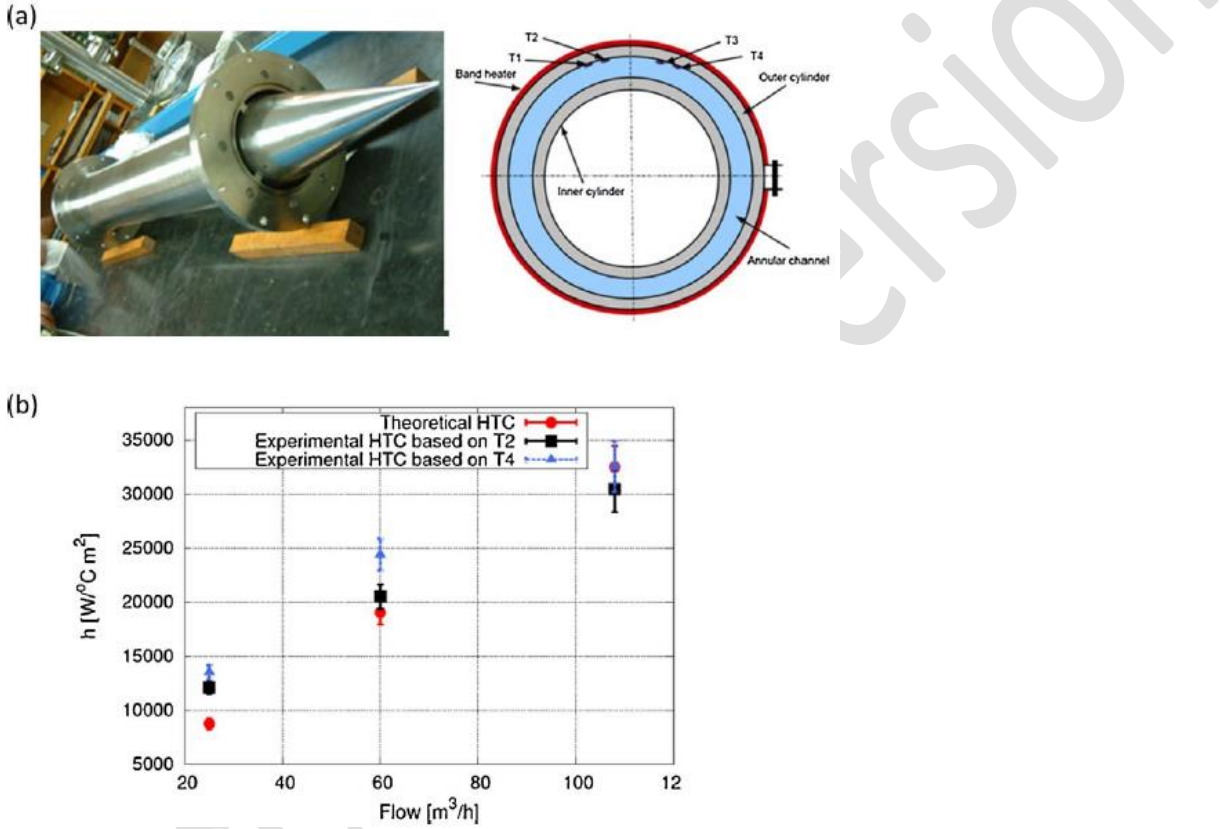

Figure 3 (a) Prototype for heat transfer measurements and cross-section showing the layout

The deuterons are stopped in the first 10 micrometers of the inner cone surface. Most of them remain at the position where they hit the beam stop but a small fraction is scattered from the surface after losing part of its energy being finally deposited in a position closer to the cone vertex. The resulting power deposition, which has conservatively been considered as a surface load, has been the input for the mechanical analyses. Sputtering has been shown not to be a problem (erosion rate has been estimated to be 8×10^{8} atoms/cm^2 leading to 2 micrometers thickness reduction after a year of full power operation).

The nominal beam power deposition profile has been obtained from the beam dynamics calculations. A thorough beam dynamics error study (with 325 beam configurations) taking into account possible deviations in the positions and currents of the magnets of the expander and transport line giving rise to beams with incorrect focusing and/or non-centered, has been performed. For thermo-mechanical analyses, the different errors have been grouped as a set of transformations of the nominal beam, varying its divergence or its axis

position or orientation in relation with the beam dump axis. It has been shown that the characteristics of the beams with errors (center, RMS size, maximum size) at the beam dump entrance are enveloped by those of a set of beams with divergences in the range ± 10%, and ± 4 mrad steer (which produces a 10 mm beam center displacement at the beam dump aperture) and therefore these have been considered to constitute the range of normal operation conditions. Fig. 4 shows the deposited power density at the inner surface of the cone for several of these beams.

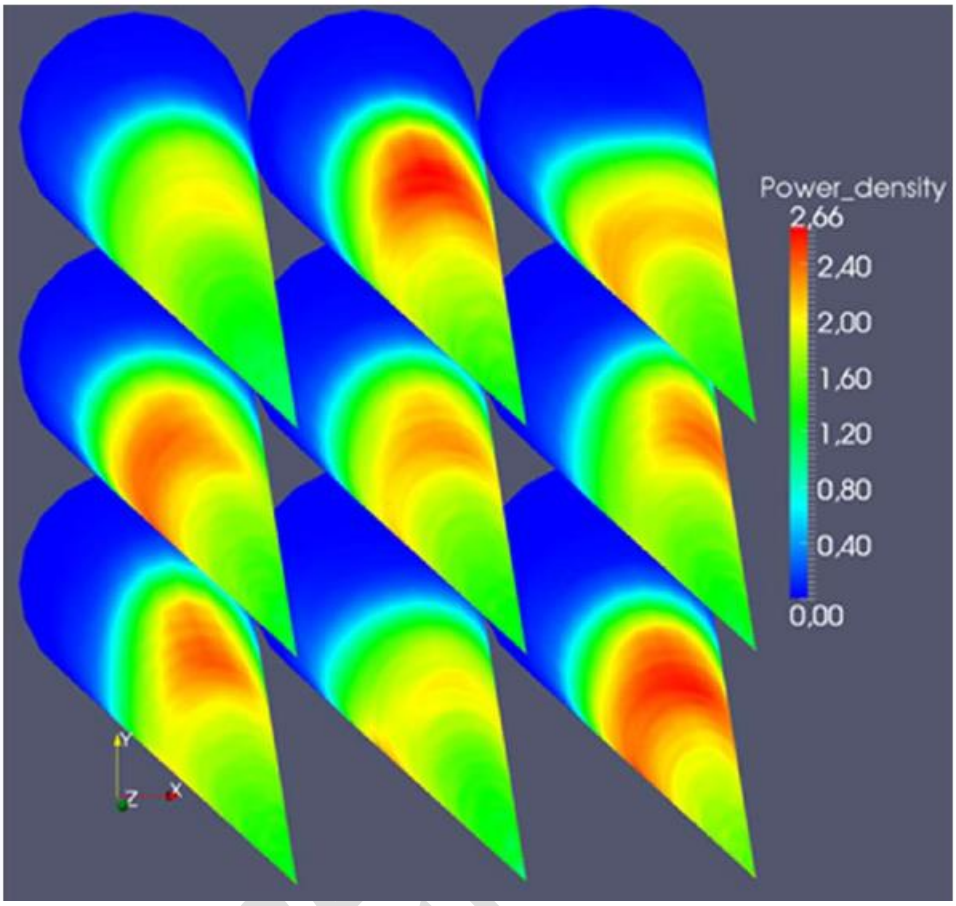

Figure 4 3D view of deposited power density (MW/m^2) for different types of beams. Left to right and top to bottom: opened beam with divergence 10% larger than nominal, beam with its axis steered 4 mrad vertically, beam with divergence 10% larger than nominal in horizontal (x) direction and 10% lower than nominal in vertical (y) direction, beam steered −4 mrad horizontally, nominal beam, beam steered 4 mrad horizontally, beam with divergence 10% lower than nominal in horizontal direction and 10% higher than nominal in vertical direction, beam with its axis steered −4 mrad vertically, closed beam with divergence 10% lower than nominal. 3D view of deposited power density (MW/m^2).

Using the ITER SDC-IC rules it has been demonstrated that the beam dump can operate in continuous mode under the loading produced by beams within this range. As an example, Fig. 5 shows the temperatures and stresses calculated in the nominal case and for a steered beam. Table 1 shows the stress limits used in the assessment. For thermal stresses the 3Sm value is used as a limit. Table 2 shows the maximum temperature, maximum stress and its location for some of the different beams analyzed. It can be observed how divergence deviations from the nominal value produce a stress increase and an axial displacement of the maximum stress location which coincides with that of the maximum power density. For steered beams the maximum stress is not located at the position of maximum power deposition but at 200 mm from the cone tip as it is observed in the example of Fig. 5.

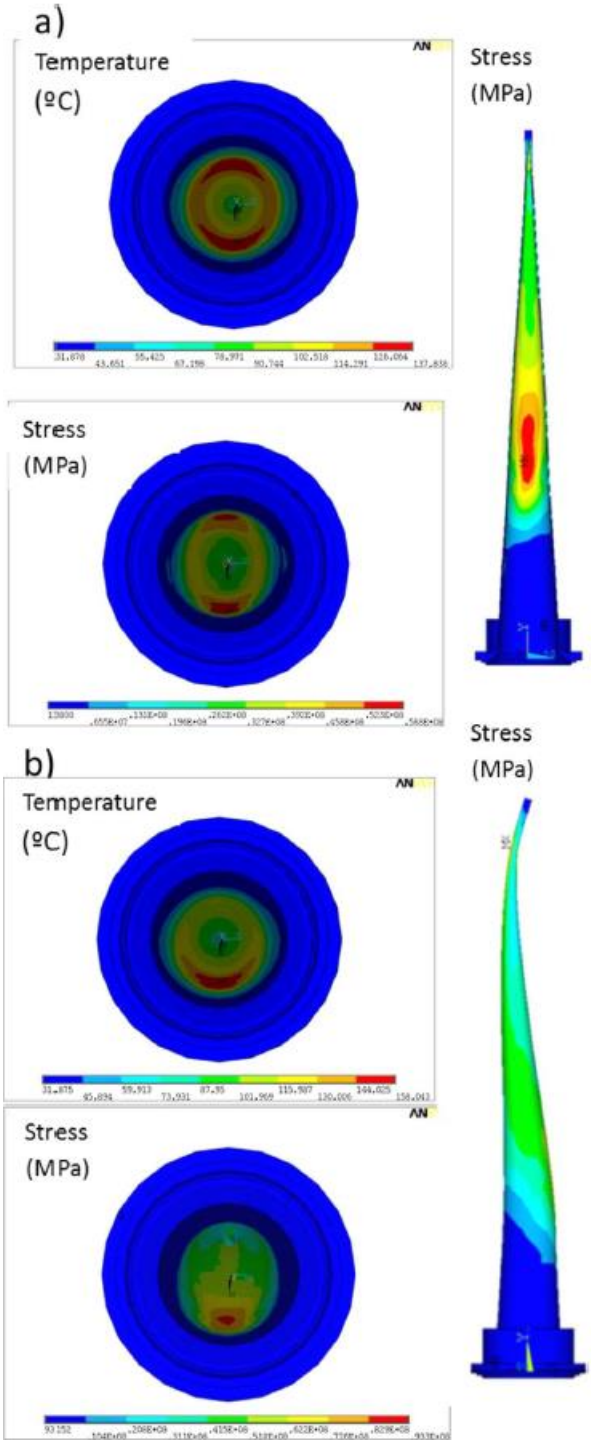

Figure 5 Temperatures (°C) and von Mises stresses (MPa) for a) the nominal case and b) for a 4 mrad steered beam.

Table 1 Experimental values of mechanical properties for electroformed copper.

	At 20 °C	At 150 °C
Yield stress σ_y, MPa	259	197
Tensile stress σ_u, MPa	316	235
S_m, MPa	105.3	78.3
$3\,S_m$, MPa	316	235

Table 2 Maximum temperatures, stresses and location of maximum stress for different beams. Normal operation range is marked in green. Red rows correspond to emergency conditions, based on material limits and yellow rows to intermediate situations.

Type of beam	Maximum internal Temperature (ºC)	Maximum external Temperature (ºC)	Maximum Equivalent stress (MPa)	Maximum stress z (mm) (z=0 at beam dump entrance)
nominal	137.78	108.69	56.4	1085
closed 10 %	145.88	112.87	68.9	1220
closed 20 %	160.42	122.17	78.8	1310
closed 30 %	187.94	142.07	94.4	1445
opened 10 %	131.79	105.85	64.1	915
opened 20 %	126.79	103.87	56.0	900
opened 30 %	123.22	101.21	133.0	50
opened_x closed_y 10 %	146.47	115.89	86.8	860
opened_x closed_y 15 %	150.53	119.45	118.0	880
opened_y closed_x 10 %	132.61	105.01	63.3	910
opened_y closed_x 15 %	137.55	108.97	83.2	850
steered_x ±4 mrad	145.22	113.83	93.1	2300
steered_x ±6 mrad	154.58	122.41	130	2300
steered_x ±8 mrad	165.67	131.40	166	2300
steered_y ±4 mrad	158.03	124.94	91.7	2300

If errors in the beam outside the normal range occur, the situation must be detected and corrective actions put in place. This is essential, given that the cartridge activation prevents any repair or maintenance operation. Although there are instruments in the transport line to characterize the beam properties, the beam dump will have dedicated diagnostics for its protection whose mission is to alert of abnormal situations leading to deviations from the nominal beam outside the normal range and to give an alarm when deviations are too large (greater than ± 30% divergence, ± 8 mrad steer) but still lower than those that would lead to mechanical failure of the cone.

The beam dump cartridge instrumentation consists of:

- Detectors of local boiling [8]. Although originally it was foreseen to install hydrophones in the return path of the water, it has been decided to install accelerometers in the outer surface of the cartridge instead, mainly to avoid the risk of leakage in the needed feedthroughs [9].

- Several radiation chambers, located also in the outer surface of the cartridge will provide an indication of off-normal beam power deposition.

They will also be used to monitor power deposition during normal operation and they will give an alarm in abnormal situations which do not lead to local boiling, like the case of a too opened beam.

The mechanical analyses have provided and/or validated the geometrical tolerances for the manufacturing of the cone. They have shown that maximum imperfections of the inner surface in the order of 0.5 mm can be tolerated and that a 1 mm radius at the tip is also acceptable.

A fatigue analysis performed for pulsed beams with 1 Hz repetition frequency and different duty cycles showed that for duty cycles lower than 50% the beam dump can withstand more than 10^7 pulses whereas the maximum number of switches-on for full power continuous operation is of the order of 6000.

2.3. Manufacturing

The manufacturing of the beam dump cone is complicated, as on one hand the result must comply with the geometrical and dimensional tolerances which are strict for such a long and thin piece and, on the other hand, the mechanical properties of the final piece must be as uniform as possible, so that welds must be avoided. The technology chosen for its production is electroforming [11,12] which provides the required tolerances with a very pure copper with good mechanical properties. It has also the advantage of being an additive technique and therefore being easily repaired and easily joined to other materials as stainless steel (this is needed at the cone flange to provide a stainless steel surface which can be used for the vacuum-tight joint to the rest of the line).

A 1:1 scale prototype has already been produced with this technique (see Fig. 6) and the final piece is presently under manufacturing. The final procedure consists on manufacturing first the tip and the flange and afterwards the rest of the cone by electrodepositing copper on a stainless steel mandrel in which the tip and flange have already been mounted. The assembly of the tip and flange on the mould must be performed with the aid of a laser tracker for obtaining the required tolerances. Fig. 7 shows this assembly and the fixture that holds it during electrodeposition avoiding deformations and allowing the rotation in the electrolytic bath.

Figure 6 Inner cone prototype and shroud.

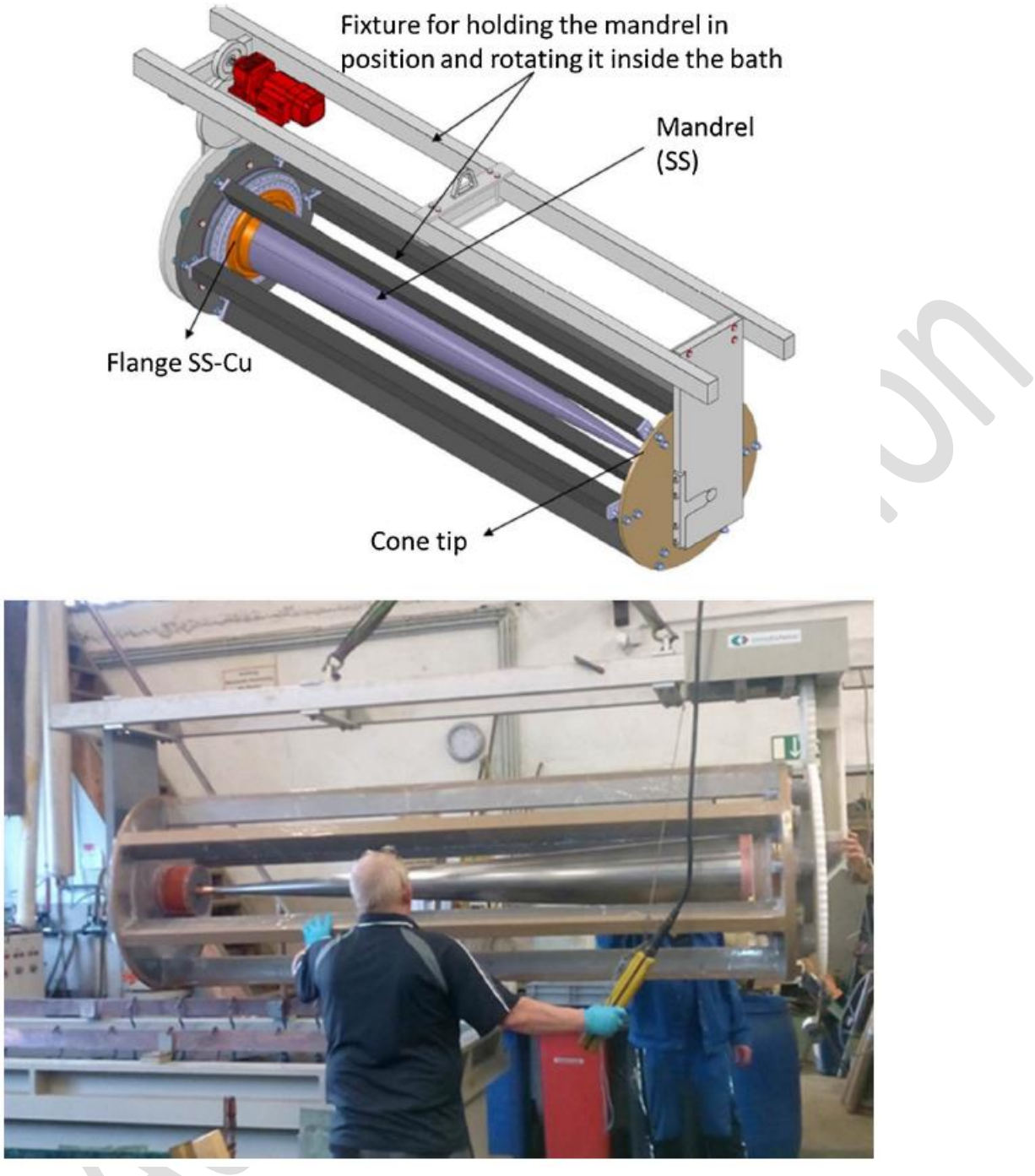

Figure 7 Assembly for electroforming of the cone body. Scheme and picture of its introduction in the electrolytic bath.

Several lessons have been learned after the prototype manufacturing, being the most important ones:

- Stainless steel is better material than aluminum for the mandrel. It does not require a metallic paint to be applied, rests of which are left in the final piece, and it has not the risk of hydrogen production leaving voids in the copper.

- Assembly of tip, flange and mandrel must be made very carefully keeping all three pieces coaxiality.

- Electrodeposition must take place in an electrolytic bath without any other pieces which could disturb the current, keeping the main parameters (bath composition, current density) under strict control

- Interruptions of the electrodeposition process must be minimized to avoid incorrect transients in the process which is not automatized

- Anisotropies in the mechanical behavior have been observed in the production of very thick pieces.

Due to this last observation, the tip piece for the final cone (see Fig. 8) has been manufactured by electro-erosion of an Oxygen-free Electronic (OFE) copper laminated bar whereas two flanges are presently being manufactured: one by electroforming and the second one from OFE copper, electron beam welded to a stainless steel ring.

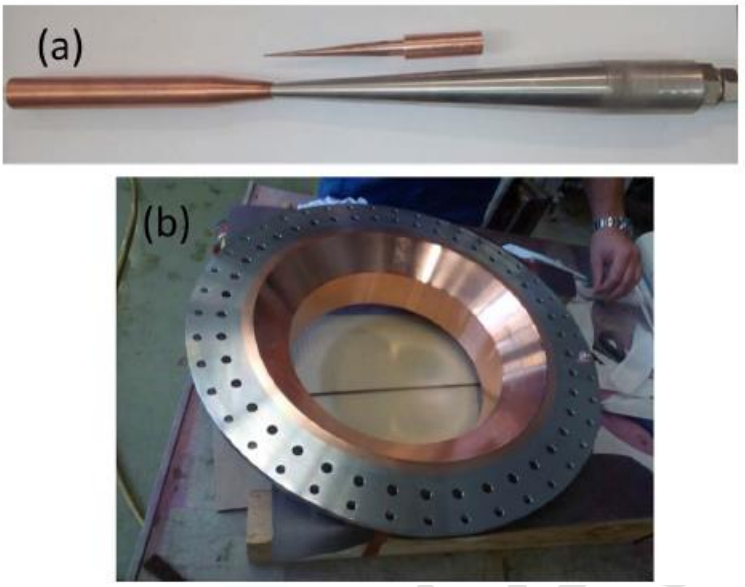

Figure 8 a) Tip produced by electro-erosion. The figure shows one of the molds used during the manufacturing process. b) Flange produced by electrodeposition.

3. Shield

Due to the interaction of the 9 MeV deuterons with the copper, both neutrons and gammas are generated. Neutrons generated from d–d reactions between beam deuterons and those which have been previously implanted in the copper, are negligible compared with the former [13]. There are not experimental values available of the total neutron and gamma production rates on copper by 9 MeV deuterons. A comparison of nuclear data libraries and experimental double differential neutron production data shows that TENDL is the most accurate data source for calculating these values [14,15]. Using these library data, the primary neutron yield per deuteron is 9.7×10^{-4} (with a mean energy of 1.8 MeV and 99 percentile at 8 MeV) whereas the primary gamma yield per deuteron is 1.9×10^{-3} (with a mean energy of 2.5 MeV and 99 percentile at 8 MeV). These particles create additional neutrons and gammas by further interactions. The spatial distribution of the primary source follows that of the beam deposition on the inner surface of the beam stopper, while the angular distribution is biased towards the deuteron beam direction.

Deuteron radiation and, to a lesser extent, neutron radiation give rise also to activation of the copper cone and therefore to residual radiation. The most relevant isotope is Zn65, with a maximum activity at the end-of-life (after 6 months integrated continuous full power operation) of 25 TBq and a half-life ($T_{1/2}$) of 245 days. Cu64 ($T_{1/2}$=12.8 h) and Ga 66 ($T_{1/2}$=9.4 h) also have a contribution to doses but only during a few days after shutdown.

To fulfill the dose limits established for the project (12.5 µSv/h for exposed workers, 0.5 µSv/h for the public) the cartridge is surrounded by a shield which has been designed to attenuate both the radiation produced during accelerator operation and the residual radiation [16,17]. This shield (see Figs. 1 and 9) is made of an inner layer of polyethylene to moderate neutrons and an outer layer of iron (to attenuate gammas produced by deuteron interactions with Cu but also those generated by neutrons in the polyethylene). In the central part surrounding the cartridge the thicknesses of the polyethylene and iron layers are 45 cm and 25 cm respectively.

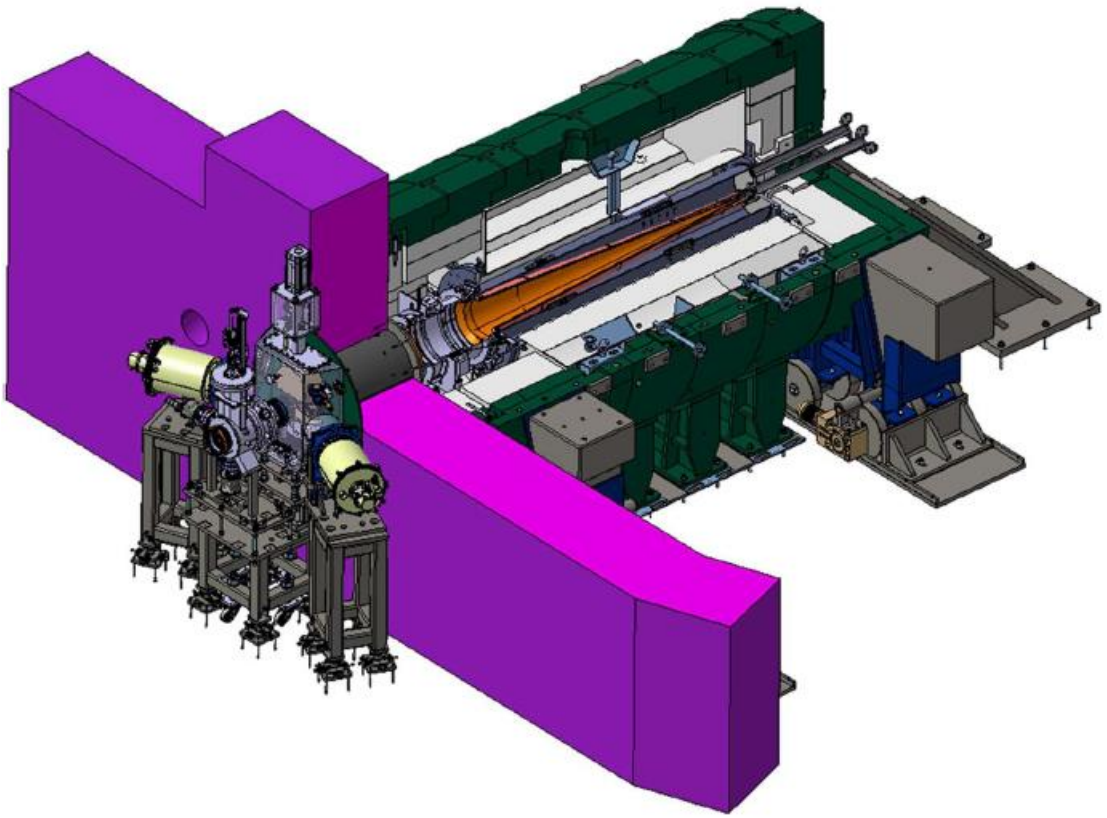

Figure 9 Quarter section of the beam dump showing all shielding elements.

At the front side (towards the accelerator), the shielding is closed with a 700 mm thick, 3 m high concrete wall which separates the space where the beam dump is located (called beam dump cell) from the rest of the vault. This wall will have a cylindrical hole for the passage of the beam tube. To minimize the radiation leakage the tube has been designed to be conical, (adjusting its diameter to the increasing diameter of the beam) and the space between wall and tube has been filled with polyethylene and lead pieces (Fig. 10). The design of this interface has been done with the criteria of allowing the assembly of the different pieces while minimizing the neutron and gamma radiation escaping through the gaps between adjacent pieces.

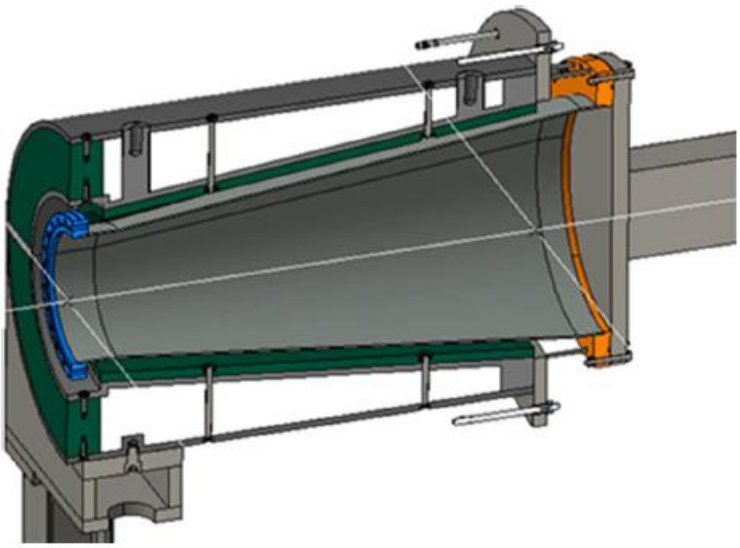

Figure 10 Detail showing the conical beam tube and shielding elements filling the space between tube and concrete wall.

Fig. 11 shows an exploded view of the beam dump shield and Fig. 12 shows some pieces already manufactured. The iron shield is made of several parts (16), all of them lighter than 4.8 ton, which is a project requirement for handling and installation. Radiation streaming is avoided by overlapping joints with a dogleg shape between adjoining pieces. All the penetrations have been designed also with this shape by the use of tailor-made inserts. The polyethylene shield is divided also in two parts to allow the cartridge removal from above. These two parts consist on two semi-cylindrical aluminum tanks which contain the polyethylene and which support the cartridge allowing its fine positioning. Aluminum has been chosen because of its low activation rate and its impurity content has been limited to avoid elements that would lead to long lived isotopes thus obviating the need of managing the tanks as a radioactive waste at the end of the facility life.

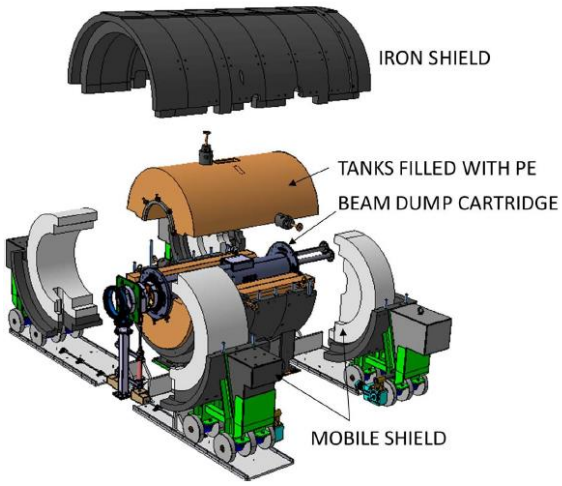

Figure 11 Parts of the Beam dump local shield.

Figure 12 Pictures of different components of the shield already manufactured.

The frontal and rear parts of the shield are mounted in trolleys which can be displaced perpendicularly to the beam dump axis to facilitate the assembly and allow access to the cartridge flanges and to the connection to the accelerator line.

Mechanical analyses of the whole shield have been implemented with Finite Element Methods in order to ensure its structural stability, following the ASME BPVC Section 8 Division II and applying seismic loads.

The aluminum tanks have two flanges where the cartridge is supported with a fine positioning system, which allows the installation of the cartridge in its nominal position with an overall accuracy of± 0.1 mm with a laser tracker. Manufacturing tolerances of the different shielding pieces, of the order of 1–2 mm, and the margins between them (radial margins of 20 mm between tanks and iron shield and of 120 mm between the cartridge

and the tanks) have been defined to ensure a positioning range of ±5 mm in radial direction and ±2.5 mm in axial direction.

The LIPAc accelerator is installed inside a vault surrounded by 1.5 m concrete walls. The shielding described above surrounds the beam dump completely except at the entrance of the beam line through the concrete wall (see Fig. 4), through which radiation escapes during operation towards the accelerator. A dipole in the last part of the accelerator bends the beam trajectory to protect the most sensitive elements – such as the superconducting linac – from this radiation. Also polyethylene pieces are placed surrounding the beam tube at different places to collimate the radiation stream. Fig. 13, which is a color dose rate map around the accelerator during full power accelerator operation, shows that the dose rates outside the accelerator vault are under the limits. It can be observed that inside the vault the main radiation source is that from the beam dump.

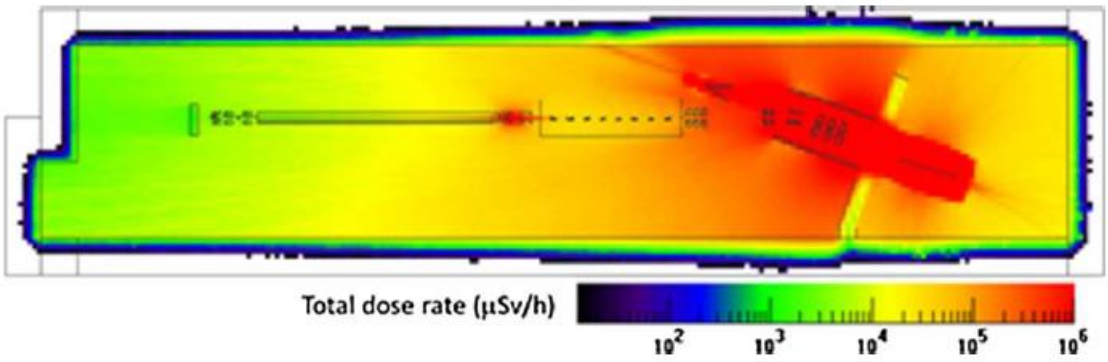

Figure 13 Total radiation dose rate map. The colored zone corresponds to dose rate values greater than the limit of 12.5 uSv/h.

A lead shutter (Fig. 14) will be inserted in the beam tube when the accelerator is switched-off to close the hole in the shield needed for the beam tube, shielding the gamma radiation coming from the activated cartridge and reducing the dose rates in the vault to values that permit hands on maintenance of the accelerator elements upstream this shutter. The shutter, 120 mm thick and with a cone frustum shape with diameters 30 cm and 42 cm, is moved by a pneumatic mechanism. The materials for this system have been carefully chosen to resist the foreseen radiation doses (up to 10^5 Gy at the actuator), and the design ensures that if a failure occurs in the compressed air supply, the shutter will be in closed position. When the lead shutter is closed the dose rates behind it at a radial distance of 40 cm from the beam axis will be lower than 10 mSv/h.

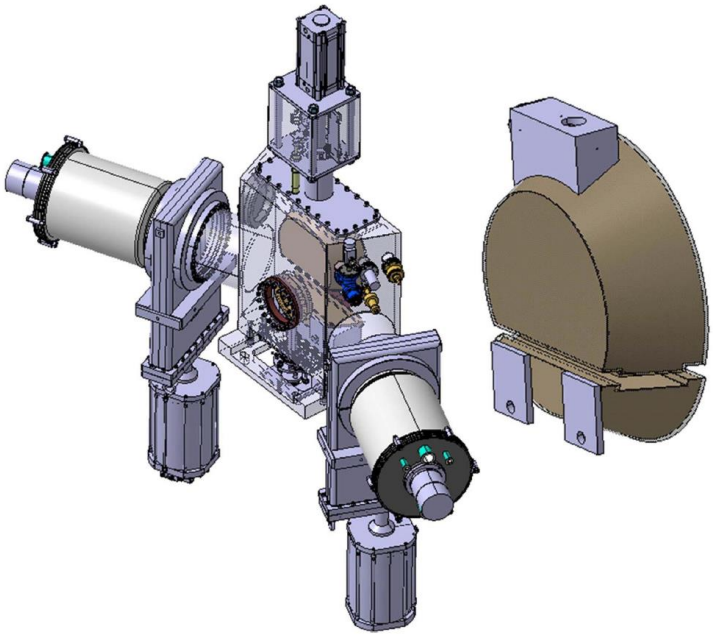

Figure 14 Lead shutter and vacuum chamber containing it.

The cartridge activation is the main cause of accelerator residual doses (there are other sources in the places where beam particle losses occur, like scrapers) and has important consequences on accelerator operation:

- During shutdown periods it is compulsory to have the full shield completely closed around the cartridge before allowing human access to the vault. This means that the PE and iron shield cannot be opened at any rate and that the lead shutter must be closed.

- Hands-on maintenance is not possible downstream the shutter (conical tube through wall, all elements inside the beam dump shield). As in LIPAc no remote handling is foreseen, a very robust design of these components has been done.

- For dismantling of the cartridge at the end of life, the operations of disconnection from the beam line, cooling pipes, etc. will be done manually from outside the closed shield. The rest of operations (removal of the upper shield and cartridge) have to be done remotely.

After dismantling, the cartridge should be introduced into a lead container and managed as a radioactive waste.

4. Cooling system

The beam dump cooling system guarantees the required parameters of water flow rate (108 m^3/h) and pressure (3.5 bar) at the beam dump entrance. For the operation at low duty cycle during commissioning and start-up, a smaller pump will be used. Most of the elements of the cooling system are located in a skid outside the accelerator vault where radiation levels are such that maintenance personnel access during operation is allowed. Those elements which necessarily must be inside the vault (temperature, pressure and flow monitors, valves, air purgers) have been located in the regions with lower radiation and where access for maintenance is possible (for example, the cartridge air purge has been located in the outlet pipe, outside the shield). A careful material selection has been done for these elements.

Required water parameters are pH between 8 and 8.5, a limited oxygen content (< 10 ppb) and conductivity in the range (0.5–2) µS/cm. The first two parameters are controlled with the aim of limiting the copper corrosion and therefore the amount of activated products in the water. These activated corrosion products

will be removed from the water loop thanks to the conductivity control. To maintain the water quality the cooling system includes a purification loop which contains a mixed resin bed, a deaerator and a NH_3 injection system. The design of the system is based on the very conservative assumption of a maximum corrosion rate of the copper of 50 mg/m^2 per day. Simulations of the circuit performed with TRACT code [18] predict a much lower corrosion rate of the order of 3 mg/m^2 per day showing that neither the cone thickness nor the cooling channel width should be affected.

The resin bed, which is located in the skid, will be surrounded by a 15 mm thick lead shroud which shields the gamma radiation caused by the impurities accumulating in it (mostly Cu64) and guarantees that the doses around it are below the limit for workers [19].

The activation of the water itself has also been studied. Tritium production in the water (from neutron reactions with oxygen and deuterium) has been estimated to be 16 Bq/cm^3 after 6 months continuous operation at full power which is under the limit established in 10-CFR of USNRC [19]. The reaction of the higher energy neutrons of the spectrum (above 10.2 MeV) with the oxygen of the water leads also to the production of N16. This isotope decays in a very short time (7.13 s) producing high energy gammas (6.13 and 7.12 MeV) which constitute the main source of radiation from the cooling water during the accelerator operation. A serpentine with a large diameter and length (volume of 1.7 m^3) has been inserted in the system with the aim of delaying the passage of the cooling water from the accelerator vault to the heat exchanger room letting the N16 enough time (57 s) for decaying [20].

The cooling circuit design includes means for a thorough elimination of air inside the water which is necessary, not only to ensure a correct heat transfer but also to avoid undesired noise on the cartridge accelerometers which could hinder the prompt boiling detection.

5. Connection to the beam line

The cartridge is connected to the rest of the accelerator through a system [21] that provides the flexibility needed for installation and alignment taking into account manufacturing and mounting tolerances and which allows its disconnection from outside the shield.

The connection of the cartridge to the beam line (see Fig. 15) is made with two bellows joined by a collar which is able to provide the required vacuum closure by tightening only two screws. The first bellow on the accelerator side is an edge-welded type to provide enough flexibility. The second bellow, which is joined to the cartridge, has been chosen to be of the hydroformed type due to its higher robustness given that, in spite of the scraper, there is small risk of beam particle losses in this part of the line if the accelerator is out of its normal operation range.

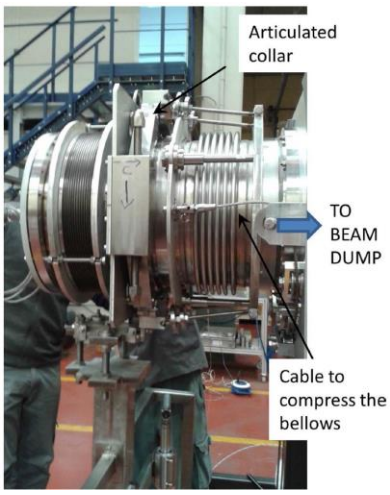

Figure 15 Connection of the beam dump to the line.

A scraper located at 1.6 m from the beam dump entrance upstream, inside the lead shutter chamber (see Fig. 14), protects the elements of the beam line inside the beam dump cell from abnormal heating, by stopping outer beam particles that could impinge on them during offnormal accelerator operation. It consists of a cooled aluminum ring with inner diameter 116 mm (see Fig. 16). It has been designed to bear a maximum continuous power of 900 W. Although the scraper should only stop particles during transient situations with off-normal beams, it has been decided to manufacture it in aluminum to minimize its activation. It will be equipped with thermocouples to provide information of the outer beam shape and/or its displacement from the center.

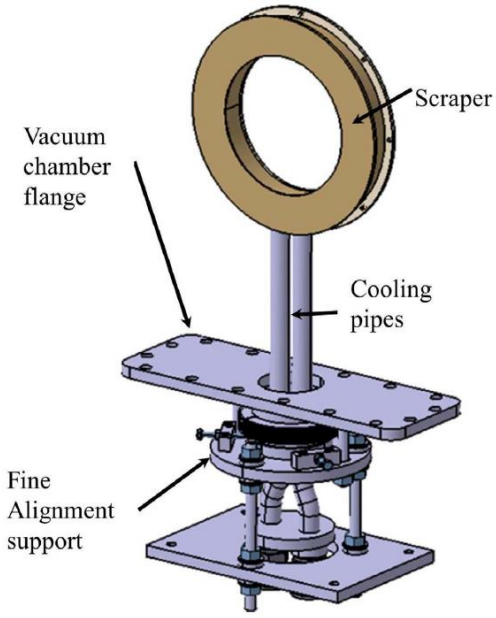

Figure 16 Scraper.

6. Summary

The last section of the LIPAc accelerator is in charge of stopping the deuteron beam once it has been diagnosed. A number of challenges are associated to the characteristics of the beam, such as high intensity, power, continuous operation, and high availability, while others derive from plant requirements involving radioprotection, installation, monitoring, investment protection, and decommissioning amongst others.

The complete design of several sub-systems of the LIPac beam dump along with the status of their manufacturing and acceptance tests has been presented. The beam dump system functions are accomplished by the following break-down structure: a cartridge incorporates the main beam facing component in charge of stopping the ion beam by means of a 2.5 m Cu cone. This element is cooled by a constant high-velocity flow of liquid water, supplied by a dedicated cooling sub-system located outside the accelerator vault. A serpentine coil delays the passage of the water through the concrete walls of the vault, letting its activity to decay. Oxygen content, pH and conductivity are controlled to minimize the corrosion of the copper cone. The neutrons and gammas generated by the nuclear interactions between the ions and the beam stopping material are moderated by dedicated shielding assemblies. The main shield surrounds the cartridge, allowing the installation and dismantling by remote means. In addition, a movable shield operating in vacuum is provided for meeting shut-down dose limits inside the accelerator vault, and specific inserts are incorporated around the accelerator tube removing any gaps between this and the wall which separates the vault and the beam dump cell. The beam dump is joined to the accelerator line by a remotely actuated flange, and a scraper in the last part of the line right before the beam dump cell protects all the downstream elements from any off-normal or fault state of the beam.

As the cartridge activation precludes any maintenance activities in the beam dump and neighboring elements downstream the lead shutter, their design and material selection are driven by a maintenance-free requirement after a short period of operations. The manufacturing is currently ongoing following quality standards and performing strict acceptance tests.

Acknowledgments

This work has been supported by the Spanish Government in the frame of the Broader Approach Agreement (Spanish BOE n14, p. 1988) and also under project FIS2013-40860-R.

The authors are indebted to CIEMAT general Workshop and the Fusion Department Workshop who have helped with the manufacturing of pieces and prototypes.

References:

[1] J. Knaster, S. Chel, U. Fischer, F. Groeschel, R. Heidinger, A. Ibarra, G. Micciche, A. Möslang, M. Sugimoto, E. Wakai, IFMIF, a fusion relevant neutron source for material irradiation current status, J. Nucl. Mater. 453 (2014) 115–119.

[2] J. Knaster, F. Arbeiter, P. Cara, et al., IFMIF: overview of the validation activities, Nucl. Fusion 53 (2013) 1–18.

[3] D. Gex, P.Y. Beauvais, B. Brañas, et al., Engineering progress of the linear IFMIF prototype accelerator (LIPAc), Fusion Eng. Des. 88 (2013) 2497–2501.

[4] B. Brañas, D. Iglesias, F. Arranz, G. Barrera, N. Casal, M. García, et al., Design of a beam dump for the IFMIF–EVEDA accelerator, Fusion Eng. Des. 84 (2009) 509–513.

[5] D. Iglesias, F. Arranz, J.M. Arroyo, et al., The IFMIF-EVEDA accelerator beam dump design, J. Nucl. Mater. 417 (2011) 1275–1279.

[6] B. Brañas, D. Iglesias, F. Arranz, J. Gómez, C. Oliver, G. Barrera, A. Ibarra, IFMIF EVEDA accelerator beam dump design, Proc of the European Particle Accelerator Conference, Genoa, Italy, 2008, p. 259.

[7] M. Parro, N. Casal, D. Iglesias, F. Arranz, B. Brañas, Design and analysis of the IFMIF-EVEDA beam dump cooling system, Fusion Eng. Des. 87 (2012) 332–335.

[8] D. Rapisarda, P. Olmos, B. Branas, F. Arranz, D. Iglesias, J. Molla, Boiling bubbles monitoring for the protection of the LIPAc beam-dump, Fusion Eng. Des. 96–97 (2015) 917.

[9] F. Arranz, P. Olmos, B. Brañas, Accelerometers data processing for boiling onset detection on the LIPAc beam stopper, Fusion Eng. Des. (2017).

[10] P. Olmos, D. Rapisarda, F. Rueda, et al., Stability of the LIPAc beam dump to vibrations induced by the cooling flow, Fusion Eng. Des. 89 (2014) 2210–2213.

[11] F. Arranz, B. Brañas, M. Busch, et al., Evaluation of the electroforming technique for IFMIF-EVEDA beam dump manufacturing, Fusion Sci. Technol. 60 (2011) 538–543.

[12] F. Arranz, B. Brañas, D. Iglesias, et al., Manufacturing prototypes for LIPAc beam dump, Fusion Eng. Des. 89 (2014) 1103–2199.

[13] J. Sanz, M. García, F. Ogando, A. Mayoral, D. López, P. Sauvan, et al., First IFMIF EVEDA radioprotection studies for the preliminary design of the accelerator beam dump, Fusion Sci. Technol. 56 (2009) 273–280.

[14] V. Blideanu, M. García, P. Joyer, D. López, A. Mayoral, F. Ogando, F. Ortíz, J. Sanz, P. Sauvan, Deuteron cross section evaluation for safety and radioprotection calculations of IFMIF/EVEDA accelerator prototype, J. Nucl. Mater. 417 (2011) 1271–1274.

[15] M. García, F. Ogando, P. Sauvan, Sensitivity to nuclear data in the radioprotection design of the LIPAc (IFMIF/EVEDA) beam dump, Fusion Sci. Technol. 62 (2012) 265–271.

[16] M. García, F. Ogando, et al., Optimized design of local shielding for the IFMIF/ EVEDA beam dump, Proc. Shielding Aspects of Accelerators, Targets and Irradiation Facilities ? SATIF 10, Geneva, Switzerland, 2010.

[17] O. Nomen, J.I. Martínez, F. Arranz, et al., Detailed mechanical design of the LIPAc beam dump radiological shielding, Fusion Eng. Des. 88 (2013) 2723–2727.

[18] M. Parro, P. Karditsas, A. Caloutsis, D. Iglesias, B. Brañas, A. Abánades, Corrosion and activation analysis of the LIPAC beam dump cooling circuit, Fusion Eng. Des. 88 (2013) 827–830.

[19] F. Ogando, P. Sauvan, D. López, J. Sanz, B. Brañas, F. Arranz, Activation analysis of the water cooling system of the LIPAc beam dump, Fusion Eng. Des. 89 (2014) 2053–2056.

[20] United States Nuclear Regulatory Commission Recommendations (USNRC-10CFR), (2017) http://www.nrc.gov/reading-rm/doc-collections/cfr/part020/appb/.

[21] F. Arranz, O. Nomen, B. Brañas, J. Castellanos, Remote disconnection system for the beam dump of the LIPAc accelerator, Fusion Eng. Des. (2017) (Sent to).